The McbB Component of Microcin B17 Synthetase Is a Zinc Metalloprotein†

Deborah B. Zamble,‡ Craig P. McClure,§ James E. Penner-Hahn,§ and Christopher T. Walsh*,‡

Department of Biological Chemistry and Molecular Pharmacology, Harvard Medical School, Boston, Massachusetts 02115, and Department of Chemistry, The University of Michigan, Ann Arbor, Michigan 48109

Received June 19, 2000; Revised Manuscript Received August 24, 2000

ABSTRACT: The microcin B17 synthetase converts glycine, serine, and cysteine residues in a polypeptide precursor into oxazoles and thiazoles during the maturation of the *Escherichia coli* antibiotic Microcin B17. This multimeric enzyme is composed of three subunits (McbB, McbC, and McbD), and it employs both ATP and FMN as cofactors. The McbB subunit was purified as a fusion with the maltose-binding protein (MBP), and metal analysis revealed that this protein binds 0.91 ± 0.17 zinc atoms. Upon incubation of MBP-McbB with excess zinc, the stoichiometry increased to two atoms of zinc bound, but metal binding to the second site resulted in a decrease in the heterocyclization activity when MBP-McbB was reconstituted with the other components of the synthetase. Apo-protein was prepared by using *p*-hydroxymercuriphenylsulfonic acid (PMPS), and loss of the metal caused a severe reduction in enzymatic activity. However, if dithiothreitol was added to the PMPS reactions within a few minutes, enzymatic activity was retained and MBP-McbB could be reconstituted with zinc. Spectroscopic analysis of the cobalt-containing protein and extended X-ray absorption fine structure analysis of the zinc-containing protein both provide evidence for a tetrathiolate coordination sphere. Site-directed mutants of MBP-McbB as well as the synthetase tagged with the calmodulin-binding peptide were constructed. Activity assays and metal analysis were used to determine which of the six cysteines in McbB are metal ligands. These results suggest that the zinc cofactor in McbB plays a structural role.

Peptide-based natural products contain a variety of remarkable structures such as the five-member heteroaromatic rings oxazoles and thiazoles (*1*). These types of heterocycles are components of a broad spectrum of therapeutic agents with a diverse array of cellular targets, including the anticancer drug bleomycin, the antiviral agent thiangazole, and the antibiotic thiostrepton. Compounds containing variations on the standard amino acids are produced in vivo by two possible pathways (*2*). Nonribosomal biosynthesis involves multidomain enzymes that piece together and modify small amino acid building blocks. The alternative is posttranslational transformation of a polypeptide precursor, a process that is limited to the genetically encoded amino acids. The biosynthesis of the *Escherichia coli* antibiotic Microcin B17 (MccB17)[1] falls into the latter category. Mature MccB17 contains oxazole and thiazole rings as well as a 4,2-fused oxazole−thiazole ring and a 4,2-fused thiazole−oxazole ring, derived from gly-ser, gly-cys, gly-ser-cys, and gly-cys-ser sequences in a peptide precursor, respectively (*3*, *4*). The genes required for MccB17 production (*mcbABCD*), export (*mcbEF*), and immunity (*mcbG*) have been identified and are all located on a single, plasmid-borne operon that is induced in the stationary phase (*5*). This system provides a singular opportunity to investigate the biological mechanism of oxazole and thiazole production in detail.

Isolation of the MccB17 synthetase revealed that it is composed of three components (McbB, McbC, and McbD) and that the enzyme assembles heterocycles in the 69-amino acid polypeptide precursor, encoded by *mcbA* (Figure 1) (*6*). The 26 N-terminal residues of McbA are required for ring formation but are removed by an unknown protease in the final step of antibiotic production (*7*, *8*). This leader sequence and the first bisheterocyclization site in $McbA_{1-46}$ provide the minimal structural elements required for synthetase activity (*6*, *9*). Biochemical analysis of mutant substrates demonstrated the significance of the distance between the leader sequence and the first enzymatic cyclization site (*9*) as well as the chemoselectivity and regioselectivity of the enzyme (*10*, *11*) and the consequences of changing the sequence context (*9*, *11*). Furthermore, an examination of the full-length McbA intermediates suggested that the synthetase is both distributive and directional, starting from the N-terminal site (*12*).

† This work was supported by NIH Grant GM 20011 to C.T.W., NIH Grant GM-38047 to J.E.P.-H., and Michigan Chemistry-Biology Interface Training Program Grant GM-08597 to C.P.M. D.B.Z. is an NIH postdoctoral fellow.

* To whom correspondence should be addressed. Phone: (617) 432-1715. Fax: (617) 432-0556. E-mail: walsh@walsh.med.harvard.edu.

‡ Harvard Medical School.

§ The University of Michigan.

[1] Abbreviations: CBP, calmodulin-binding peptide; dNTP, deoxynucleotide triphosphate; DTNB, 5,5′-dithiobis(2-nitrobenzoic acid); DTT, dithiothreitol; EDTA, ethylenediaminetetraacetic acid (disodium salt); EXAFS, extended X-ray absorption fine structure; Hepes, 4-(2-hydroxyethyl)-1-piperazineethanesulfonic acid; HPLC, high-pressure liquid chromatography; HRP, horseradish peroxidase; ICP, inductively coupled plasma; IPTG, isopropyl 1-thio-β-D-galactoside; MBP, maltose-binding protein; MccB17, microcin B17; MS, mass spectrometry; PAGE, polyacrylamide gel electrophoresis; PAR, 4-(2-pyridylazo)resorcinol; PCR, polymerase chain reaction; PMPS, *p*-hydroxymercuriphenylsulfonic acid; Tris, tris(hydroxymethyl)aminomethane; wt, wild-type; XAS, X-ray absorption spectroscopy.

10.1021/bi001398e CCC: $19.00
Published on Web 11/29/2000

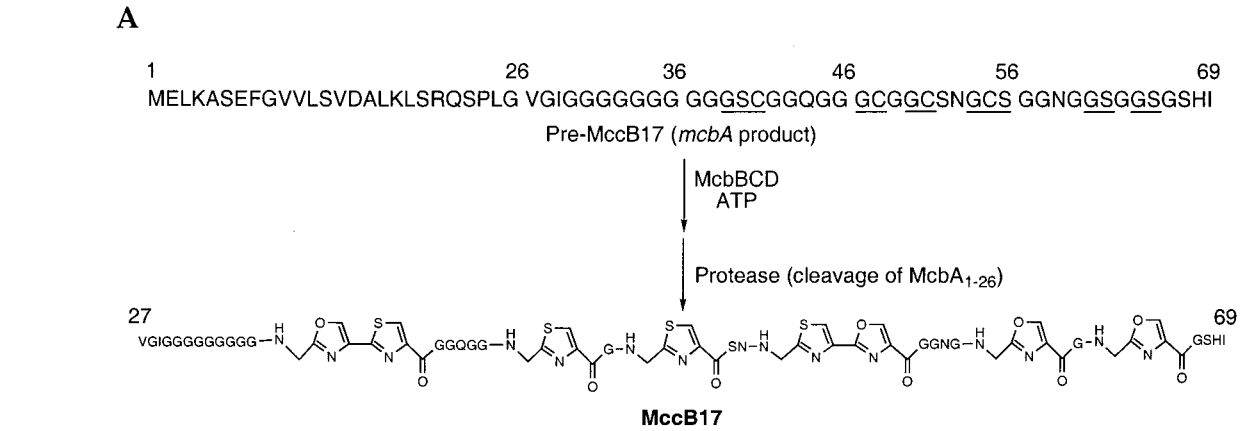

FIGURE 1: Maturation of MccB17. The 69-residue peptide encoded by *McbA* is processed by McbB, McbC, and McbD to produce eight heterocycles at the underlined residues. The N-terminal 26 amino acids are removed by an unidentified *E. coli* protease to release mature antibiotic.

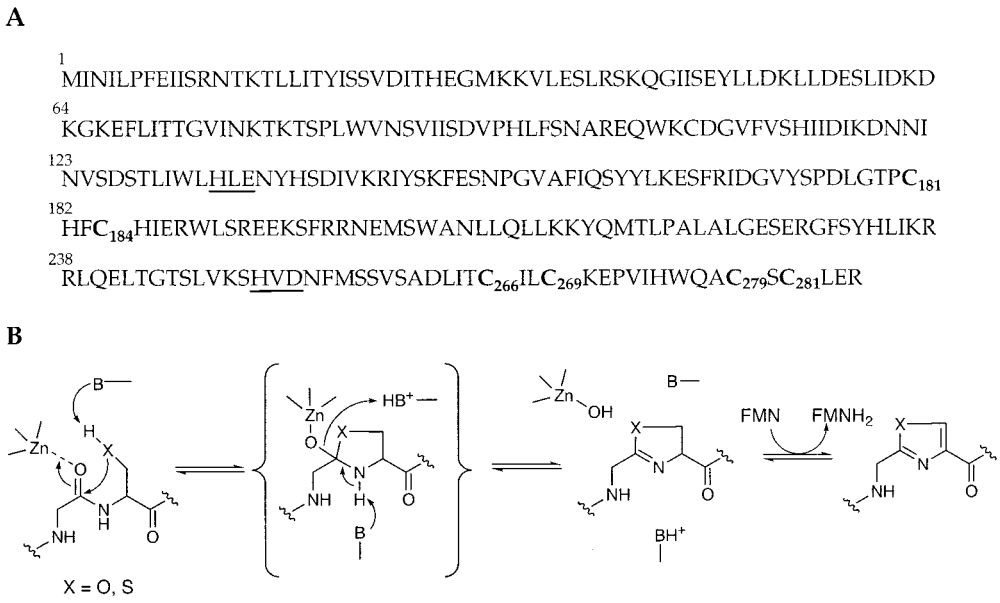

FIGURE 2: (A) Primary sequence of McbB. The cysteine residues are numbered. The underlined HxE and HxD sites are a part of the motifs similar to the HxE.....CxxC sequence that is found in cytidine deaminase, in which the cysteine and histidine residues are zinc ligands and the glutamate is a proton shuttle. (B) Proposed mechanism of synthesis of oxazoles and thiazoles by the MccB17 synthetase. A possible role for zinc is shown.

The initial search for synthetase cofactors revealed a requirement for ATP or GTP (*6*), and subsequently it was shown that NTP hydrolysis is dependent on the presence of a cyclizable substrate (*13*). The subunit McbD contains several motifs homologous to ATP- and GTP-utilizing enzymes, and mutagenesis at some of these sites reduced microcin production both in vivo and in vitro, suggesting that McbD is the conditional ATPase component of the enzyme (*13*). No ATPase activity of McbD was detected in the absence of McbB or McbC (*13*). The presence of a second cofactor was indicated by the yellow color of McbC, a consequence of stoichiometric, noncovalently bound FMN (*6*, *14*).

Preliminary characterization of McbB as a metalloprotein was prompted by two CxxC motifs with limited homology to cytidine deaminase (Figure 2A) (*14*). The catalytic zinc in that mononuclear enzyme is coordinated by the two cysteine residues in a CxxC motif and a histidine in an upstream HxE sequence (*15*). The fourth ligand at the cytidine deaminase metal site, water, is deprotonated by the proximate glutamate in the HxE sequence, and the resulting hydroxide is activated to attack cytidine (*15*). The reverse of this reaction corresponds to a proposed mechanism for heterocycle formation (Figure 2B). In analogy with cytidine deaminase, the zinc of McbB could activate the carboxyl group upstream from the ring-forming cysteine or serine for nucleophilic attack, stabilize the tetrahedral intermediate, and accept the leaving hydroxide anion. Such a role for McbB in the dehydration reaction is reminiscent of many other zinc-containing enzymes (*15*).

All three synthetase components are required to modify the McbA substrate (*5*, *6*), and there are no reported activity assays for the individual proteins. To characterize further the synthetase subunits and their cofactors, it is necessary to be able to purify the proteins separately and reconstitute activity. This goal was achieved by expressing McbB, McbC, and McbD as fusion proteins with the maltose-binding protein (MBP) (*14*). Following affinity chromatography and thrombin digestion to liberate free McbD from the MBP fusion, mixing the three subunits together resulted in heterocyclization, although with a specific activity significantly less than that of the wild-type synthetase (*14*). Thus,

it is now possible to test whether modifications of the isolated components affect synthetase activity and consequently to understand the function of each subunit. The long-term objective of obtaining such knowledge would be to apply it in the biosynthesis of new, medically useful compounds. Drugs containing oxazole and thiazole rings could interact with DNA gyrase, the putative target of MccB17 (*16*), as well as the clinically successful quinolone antibacterial drugs. In addition, potential targets include the wide variety of biological macromolecules affected by compounds containing these functional groups (*1*).

In the studies described here, we have focused on the role of zinc in MccB17 synthetase-catalyzed oxazole and thiazole formation. We investigated the stoichiometry of zinc in MBP-McbB and the metal requirements for activity. In addition, mutagenesis, metal-replacement studies, and spectroscopy were used to identify the zinc ligands. These studies suggest that the metal has a structural role and provide some insight into the MccB17 synthetase mechanism of action.

EXPERIMENTAL PROCEDURES

Materials. Competent *E. coli* BL21(DE3) and thrombin were obtained from Novagen. Competent *E. coli* DH5α were purchased from Gibco BRL. Protease inhibitors were purchased from Roche Molecular Biochemicals. Restriction endonucleases, T4 DNA ligase, and amylose resin were obtained from New England Biolabs. Calmodulin affinity resin and *Pfu* DNA polymerase were purchased from Stratagene. Oligonucleotide primers were obtained from Integrated DNA technologies. *p*-Hydroxymercuriphenylsulfonic acid (PMPS), 4-(2-pyridylazo)resorcinol (PAR), benzamidine, and 1,10-phenanthroline were purchased from Sigma. All water was deionized on a Milli-Q water system (Millipore), and the pH of all Tris buffers was adjusted with HCl.

Mutagenesis. Preparation of plasmid DNA was performed by using a QIAprep spin miniprep kit (Qiagen). Gel purification of DNA fragments and purification of PCR reaction products were performed by using a QIAquick spin kit. Construction of the expression vector for MBP-McbB, pETMBP-McbB, was previously described (*14*). Mutants were prepared by using the QuikChange site-directed mutagenesis kit (Stratagene). The primers used were 5′-cagtaatgcccgggcacaatggaaatctgatgg (E102A), 5′-cactaatctggttacatctcgcaaactatcattcagac (E135A), 5′-cactaatctggttacatctcgacaactatcattcagac (E135D), 5′-cacctgtattttagctaaagagccggtaattcactggc (C269A), 5′-ctgatcttggtgctccctgccatttttgtcatatag (T179A), 5′-ggtaattcactggcaggctgccagctgtctggagag (C279A), 5′-caggctgcagcgctctggagagataagg (C281A), and the corresponding reverse-complementary fragments. Other MBP-McbB mutants used in this study were prepared by J. C. Milne. Construction of the expression vector for CBP-tagged Microcin B17 synthetase, pCalBCDn, was previously described (*9*). The pCalBCDn plasmid was mutated in the McbB gene by using the splicing by overlap extension method (SOE). The outside primers used were 5′-gggaattgtgagcggataacaattcccctc and 5′-caagaggtaccgcggacacgaaagttcgttc. The inside primers used were the C269A and E135 primers listed above as well as 5′-cctgatcttggtactcccgcccatttttgtcatatag (C181A). All mutants were verified by DNA sequencing using dye-labeled dideoxyterminators on an Applied Biosystems model 373 or 377 instrument (Molecular Biology Core Facilities, Dana-Farber Cancer Institute).

Overexpression and Purification of MBP-McbB. BL21-(DE3) *E. coli* were freshly transformed with pETMBP-McbB, plated onto LB-agar plates containing 100 μg/mL ampicillin, and then subcloned. Overnight cultures were used to inoculate LB-ampicillin (10 mL/1 L) which was grown to an OD_{600} of 0.7−0.9 at 37 °C. The cells were induced with 1 mM IPTG and grown for an additional 3 h. In some preparations, the temperature was reduced to 30 °C during the induction period with no significant change in protein yield. The cells were harvested by centrifugation and resuspended in buffer A (20 mM Tris, pH 7.5, 200 mM NaCl, 1−2 mM DTT) containing 1.25 mM Pefabloc SC and 1 μg/mL aprotinin, chymostatin, and leupeptin. All subsequent steps were performed at 4 °C. The cells were disrupted twice in a French pressure cell (18 000 psi), and cellular debris was removed by centrifugation at 35000 rpm for 35 min in a Ti45 ultracentrifuge rotor. The supernatant was applied to an amylose column (≈5 mL resin/L of cultured cells) preequilibrated with buffer A. The column was washed with 20 column volumes of buffer A, and then the protein was eluted with buffer A containing 10 mM maltose. Fractions were analyzed by 10% SDS−PAGE, and those containing MBP-McbB were pooled, concentrated in Centriprep-30 concentrators (Millipore), and dialyzed against 20 mM Tris, pH 7.5, and 30 mM NaCl. The protein was then loaded onto MonoQ or HiTrap Q FPLC columns (Pharmacia) preequilibrated in 20 mM Tris, pH 7.5, and 30 mM NaCl. Protein was eluted with a linear NaCl gradient, and the fractions were analyzed by 10% SDS−PAGE. The fractions containing MBP-McbB were pooled, concentrated in Centriprep-30 concentrators, washed with 20 mM Tris, pH 7.5, to reduce the NaCl concentration to approximately 55 mM, frozen in N_2(l), and stored at −80 °C. During elution from the anion-exchange column, the protein separated into several distinct fractions, although they all produced bands of the same mobility on SDS−polyacrylamide gels (data not shown). Some of this protein had low or undetectable activity in the reconstitution assay as well as variable zinc content, suggesting that this fraction contained McbB protein that was not correctly folded. The extinction coefficient was estimated to be 14 1650 M^{-1} cm^{-1} at 280 nm by quantitative amino acid analysis (Brigham and Women's Hospital, Biopolymer Lab). The MBP-McbB mutants were purified in the same manner, and some of the inactive proteins eluted from the anion-exchange column at the same time as the inactive wild-type protein described above, again suggesting that the protein was not correctly folded.

Other Proteins. Fusion proteins of the other synthetase subunits, MBP-McbC and MBP-McbD, were expressed and purified as described (*14*) (F.H. and C.T.W., manuscript in preparation). The substrate used in the Western blot assays was MBP-$McbA_{1-46}$(GGC), ("GGC"), an S40G variant of $McbA_{1-46}$ that contains a single site for heterocycle modification (*11*). Overexpression and purification of the CBP-tagged synthetase was described previously (*9*).

DTNB Assay. Reactions contained 6 M guanidine hydrochloride, pH 7.2, 0.18−0.3 mM 5,5′-dithiobis(2-nitrobenzoic acid) (DTNB, Sigma), and a constant amount of protein buffer. The reactions were prepared at room temperature, and the absorbance was measured at 412 nm. A standard curve was prepared with freshly diluted β-mercaptoethanol each time the assay was performed.

Metal Analysis. All flasks and beakers were rinsed with 20% HNO_3 and Milli-Q water. Dialysis was performed in Teflon beakers, and slidalyzers (Pierce) were presoaked in 20 mM Hepes, pH 7.5, containing 10 g/L Chelex-100 (Bio-Rad). The standard method was dialysis of the proteins against four changes of 50 mM Hepes, pH 7.5, with 25−50 g/L Chelex-100 in the beaker, over a period of 18−24 h at 4 °C. All pipet tips and eppendorf tubes were rinsed with water treated with 50 g/L Chelex-100. Proteins were frozen in N_2(l) and stored at −80 °C. Metal content was determined by using either a Jarrell-Ash 965 inductively coupled plasma (ICP) emission spectrometer with a program to analyze for 20 elements or a VG PlasmQuad 3 ICP-mass spectrometer with a program to analyze for zinc and cobalt (Chemical Analysis Laboratory, University of Georgia, Athens, GA).

Western Assay for Synthetase Activity. Reaction mixtures contained 50 mM Tris, pH 7.5, 100 mM NaCl, 20 mM $MgCl_2$, 2 mM ATP, 10 mM DTT, and 20 μM GGC unless otherwise noted. Reactions with the CBP-tagged synthetase typically contained 0.05 mg/mL enzyme. To reconstitute activity from individual subunits, the MBP tag was first cleaved from MBP-McbD in a thrombin digest containing 20 μM MBP-McbD and 5.6 U/mL thrombin (Novagen), in the buffer supplied by the manufacturer at room temperature (22−24 °C) for 15 min. The digest was stopped by adding benzamidine to a final concentration of 2 mM and incubating an additional 5 min. Reconstitution assays contained the buffer described above, 2 mM benzamidine, 4 μM digested MBP-McbD, 4 μM MBP-McbB, and 4 μM MBP-McbC unless otherwise noted. Both the CBP-tagged synthetase and the reconstituted synthetase reactions were incubated at 37 °C. Aliquots were removed at the indicated time, quenched with an equal volume of SDS−PAGE loading buffer (100 mM Tris, pH 6.8, 1.8% SDS, 10% glycerol, 0.05% bromophenol blue, 5% β-mercaptoethanol), and loaded onto 10% SDS−polyacrylamide gels. The proteins were transferred to Immobilon-P PVDF membrane (Millipore) by electroblotting at 60 V for 75 min and probed with rabbit polyclonal anti-MccB17 antibodies specific for oxazoles and thiazoles (*17*). The membranes were then probed with goat anti-rabbit horseradish peroxidase-conjugated IgG (Pierce), followed by the chemiluminescent SuperSignal detection system (Pierce) diluted 1:5 in water. The membranes were exposed to film that was then developed, scanned, and quantified by using NIH image software.

PAR Assay. Zinc content was also determined by using a spectroscopic assay based on the absorption change at 500 nm associated with the formation of a zinc complex with 4-(2-pyridylazo)resorcinol (PAR) (*18*, *19*). The protein-bound zinc was released by the addition of PMPS (*18*−*20*). Adventitious metals were removed from MBP-McbB by dialysis as described above. The reactions were performed in 20 mM Tris, pH 7.5, and 55 mM NaCl that was treated with 50 g/L Chelex-100 and filtered. The reactions contained 9.1 μM MBP-McbB, 100 μM PAR, and increasing amounts of PMPS. This assay was performed at room temperature. The absorption at 500 nm was measured, and the concentration of zinc was determined by using a standard curve that was prepared with zinc atomic absorption standards (Sigma).

Preparation of apo-MBP-McbB. Initial attempts to prepare apo-MBP-McbB, performed by adding a 100 mM stock of 1,10-phenanthroline dissolved in ethanol to protein solutions and incubating on ice, suggested that inactivation of McbB was very slow. To prepare apo-protein, MBP-McbB was dialyzed against four changes of 1 mM 1,10-phenanthroline in 50 mM Hepes, pH 7.5, at 4 °C over a period of 6 days followed by several changes of Hepes buffer containing 50 g/L Chelex-100 over an additional day. Samples were prepared for metal analysis as described above. To prepare apo-protein in a shorter time frame (*20*, *21*), MBP-McbB in 20 mM Tris, pH 7.5, and 55 mM NaCl was incubated with 6 molar equiv of PMPS for 15 min on ice. An additional 10 equiv of PMPS was added as well as 2 mM EDTA, and the reactions were incubated for 15 min at room temperature. DTT was added to a final concentration of 2 mM followed by a further 10-min incubation at room temperature. The incubation times were shortened for some experiments as noted. The samples (0.3−2 mL) were dialyzed at 4 °C into 500 mL of buffer (50 mM Hepes, pH 7.5, 2 mM DTT, 1 mM EDTA 20−25 g of Chelex-100) that was changed 5 times over a period of 7−8 h. DTT was omitted from the buffer after the first two buffer changes, and EDTA was omitted from the final two buffer changes. Samples were removed from the dialysis as described above for metal analysis.

Preparation of Co-MBP-McbB. Baffled glass flasks were soaked for several days in 20% nitric acid, rinsed with freshly deionized water, and sterilized by autoclaving. The MM9 media (100 mM Pipes·NaOH, pH 6.8, 15 mM $(NH_4)_2SO_4$, 8.5 mM NaCl, 0.17 mM KH_2PO_4, 2% glucose) was treated with Chelex-100 and sterile filtered. Stocks of $MgSO_4$ and ampicillin were prepared with Chelex-treated water, sterile filtered, and added to the media at final concentrations of 1 mM and 100 μg/mL, respectively. A solution of $FeSO_4$ (Fluka) was freshly prepared in Chelex-treated water and added to the media at a final concentration of 0.5 μg/mL. Small cultures (80−100 mL) were inoculated with a single colony of BL21(DE3) transformed with pETMBP-McbB, grown for 24 h at 37 °C, and used to inoculate 1-L cultures. The cells were grown at 37 °C until the OD_{600} was 0.6−0.8, which took about twice as long as in LB. IPTG (1 mM) and 10 μM $CoCl_2$ (Sigma), both prepared in Chelex-treated water, were added and the cells were grown for an additional 3 h. Protein purification was performed as described above.

XAS Sample Preparation, Data Collection, and Analysis. MBP-McbB samples were dialyzed to remove adventitious metals as described above for metal analysis, against 50 mM Hepes, pH 7.5 (samples 1 and 2) or 30 mM Tris, pH 7.5 (sample 3) containing Chelex-100. The samples were concentrated in Centricon-30 concentrators (Millipore) prerinsed with Chelex-treated water. Glycerol (10%) was added to each sample as a cryoprotectant, and then the samples were placed in Lucite cuvettes (3 × 2 × 25 mm) with 40 μm Kapton windows and frozen in N_2(l).

XAS spectra were collected at SSRL, on beamline 9−3, under dedicated conditions (70 mA, 3.0 GeV) using a Si(220) double-crystal monochromator with a focusing mirror. X-ray energies were calibrated by simultaneous measurement of the absorption spectrum of a zinc foil, with the first inflection point assigned as 9659 eV. Samples were held at 10 K during data collection using a helium flow cryostat. Spectra were measured using 10 eV steps in the preedge region, 0.3 eV steps in the edge region (9645−9690 eV), and 0.05 $Å^{-1}$ in the EXAFS region with integration times of 1 s, 1 s, and

k^3-weighted times from 1 to 20 s, respectively, for a total measurement time of ca. 35 min/scan. Data were measured as fluorescence excitation spectra, using a 30-element Ge solid-state detector array equipped with a 3-μm copper filter and Soller slits focused on the sample. The incident count rate for each channel was held below 120 kHz to avoid saturation; the windowed Zn Kα count rate was 15−20 kHz in the EXAFS region, giving a total of approximately 8×10^6 useful counts per scan at $k = 13$ Å^{-1}. Each channel of each scan was examined independently for glitches (sharp discontinuities caused by multiple reflections from the monochromator crystals). Good channels (25−26 per scan) were then averaged for each sample to give the final spectrum.

The EXAFS data were extracted using a two-region cubic spline above the edge, followed by normalization to a Victoreen polynomial (*22*). Data were converted to k space, $k = [2m_e(E - E_o)/h^2]^{1/2}$, using $E_o = 9675$ eV. Fourier transforms were calculated using k^3-weighted data over a k range of 2.0−12.5 Å^{-1}.

EXAFS data $\chi(k)$ can be described by eq 1, where N_s is the number of scatterers at a distance R_{as}, $A_s(k)$ is the effective backscattering amplitude, S_{as} is a scale factor, σ^2_{as} is the mean-square deviation in R_{as}, $\phi_{as}(k)$ is the phase-shift that the photoelectron wave undergoes in passing through the potentials of the absorbing and scattering atoms, and the sum is taken over all scattering interactions:

$$\chi(k) = \sum_S \frac{N_s A_s(k) S_{as}(k)}{kR_{as}^2} \exp(-2k^2 \sigma_{as}^2) \sin(2kR_{as} + \phi_{as}(k)) \quad (1)$$

Experimental data were fit ($k = 2$−12.4 Å^{-1}) with theoretical EXAFS amplitude and phase functions, $A_s(k)$ and $\phi_{as}(k)$, calculated using FEFF 6.01 (*23*, *24*). Single scattering parameters were calculated for Zn−N and Zn−S using bond lengths of 2.05 and 2.35 Å, respectively. The scale factors $S = 1.02$ (S) and 0.85 (N) and threshold energy $E_o = 9$ eV were calibrated by fitting EXAFS data for crystallographically characterized zinc models (*25*). R and σ were varied, and N was held fixed at reasonable integer values. The data were analyzed as previously described (*25*).

RESULTS

Zinc Stoichiometry in McbB. The observation that McbB contains two sequence motifs with a resemblance to the active site of cytidine deaminase suggested that McbB has two putative zinc-binding sites and preliminary metal analysis established the presence of zinc (*14*). In the studies reported here, multiple MBP-McbB protein samples, prepared under several different conditions, were analyzed for zinc content by using two different ICP techniques (see Experimental Procedures). These experiments revealed that MBP-McbB binds zinc with a stoichiometry of 0.91 ± 0.17 (Table 1). Initial preparations of MBP-McbB were expressed in media supplemented with zinc sulfate; however, this addition was not required to obtain wild-type protein containing zinc so it was omitted from the majority of experiments described here.

A spectroscopic assay with the metallochromic indicator PAR was also used to measure metal content. Upon addition of the organomercurial compound PMPS to trap the cysteine thiol groups by mercuration, the zinc was displaced from MBP-McbB into solution where it formed the orange Zn−PAR complex (Figure 3). The color change was immediately visible upon mixing the solutions, and the corresponding absorbance at 500 nm was measured several minutes later and did not change over a period of hours (data not shown). Incubation of MBP-McbB alone with PAR did not cause a significant change in the absorbance at 500 nm (data not shown). Six equivalents of PMPS were required to release 10.1 μM zinc from 9.1 μM MBP-McbB. Adding more PMPS did not significantly change the concentration of the Zn−PAR complex, 10.7 μM zinc was detected after the addition of 15 equiv of PMPS. There are no cysteines in the MBP portion of the fusion protein, so all six cysteine residues of McbB must be accessible to form a PMPS−mercaptide bond, and at least one of the cysteines is a metal ligand. ICP metal analysis of the same protein sample detected 0.9 equiv of zinc.

Recent studies demonstrated that active MccB17 synthetase can be reconstituted from McbB, McbC, and McbD individually expressed as MBP fusions (*14*). Heterocycle

Table 1: Analysis of MBP-McbB Mutants[a]

MBP-McbB	% Zn[b]	free S[c]	activity[d]
WT	91 ± 17 (26)	5.4 ± 0.7 (7)	+
C181A	24 ± 11 (3)	1.4	−
C184A	29 ± 12 (2)	2.2	−
C181A/C184A	30 ± 8 (2)	1.1	−
C269A	90	5.4[e]	+
C279A	13 ± 1 (2)	2.6	−
C281A	32 ± 20 (2)	2.8	−
E102A	75	6.1	+
H133A	16	2.2	−
E135A	41 ± 14 (5)	2.6 ± 1.2 (2)	−
E135D	26	2.8	−
T179A	52 ± 11 (2)	2.8	−

[a] If more than one experiment was performed, the number of experiments done is indicated in parentheses and the standard deviation is listed. [b] Samples were dialyzed extensively in 50 mM Hepes, pH 7.5, over Chelex-100 prior to ICP metal analysis. [c] The number of free thiols was assayed with DTNB in 6 M guanidine hydrochloride, pH 7.2, and the absorbance at 412 nm was compared with a standard curve prepared with β-mercaptoethanol. [d] The activity of the MBP-McbB proteins was tested as described in Experimental Procedures. The reactions were typically incubated for 1 h at 37 °C, although a few of the mutants were also allowed to react for 21 h. [e] In the experiment to assay the free thiols of C269A, 6.2 thiols were detected in the wild-type sample.

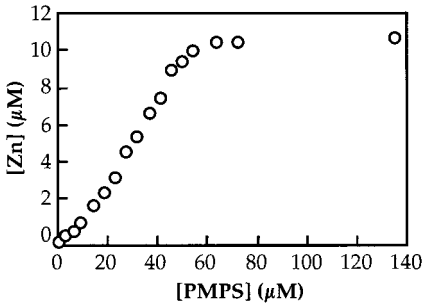

FIGURE 3: PMPS-induced release of zinc from MBP-McbB. The reactions were performed with 9.1 μM protein in 100 μM PAR, 20 mM Tris, pH 7.5, and 55 mM NaCl. For each sample the absorbance at 500 nm was measured twice and averaged. The concentration of zinc was determined by using a standard curve prepared under the same buffer conditions.

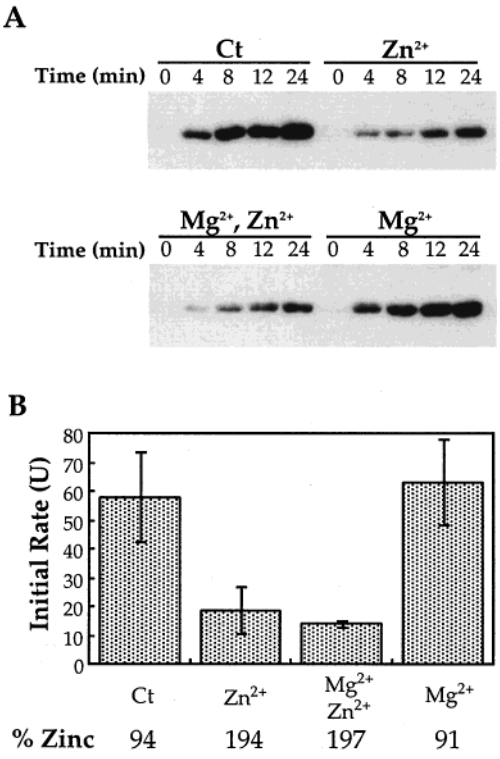

FIGURE 4: Inhibition of MBP-McbB by excess zinc. Protein samples were incubated for 1 h on ice with 2 molar equiv of zinc sulfate and/or 10 mM magnesium acetate prior to metal-free dialysis. (A) The activity of the McbB samples was tested in reconstitution assays containing 4 μM each of MBP-McbB, MBP-McbC, and thrombin-cleaved MBP-McbD, and 20 μM GGC. The reactions were incubated at 37 °C; aliquots were removed at the times indicated, resolved on 10% SDS−polyacrylamide gels, and analyzed by Western blotting. (B) The initial rate of heterocycle formation was determined over a period of 12 min for each sample of MBP-McbB. The error bars indicate the standard deviation between duplicate Western blots, such as those shown in panel A. The metal content of each MBP-McbB sample is shown and was determined by ICP emission spectrometry.

formation in the McbA substrate can be monitored by using Western assays probed with a polyclonal antibody specific for oxazoles and thiazoles (*6*). The reconstituted synthetase has a lower specific activity than the enzyme isolated as a complex, which is probably due to interference by one or more of the MBP tags or some population of misfolded protein (*14*). However, this system provides a means to correlate the metal content of McbB with activity. Incubation of MBP-McbB with 2 equiv of zinc sulfate followed by extensive dialysis to remove weakly bound metals raised the zinc stoichiometry from one to two (Figure 4). Similar levels of zinc (two/MBP-McbB) were also obtained upon incubation with 1 or 3 equiv of zinc sulfate (data not shown). These experiments suggest that there is a second, weaker zinc-binding site on McbB. Reconstitution with the other enzyme components, however, demonstrated that the increase in the amount of zinc bound to MBP-McbB caused a significant decrease in the rate of heterocycle formation (Figure 4). It is possible that the second zinc is blocking a site that is usually filled by a different metal and thereby reducing activity. For example, the *E. coli* primase can be reconstituted by 2 equiv of zinc, but in the presence of magnesium acetate only a single zinc atom was bound (*21*). In an analogous experiment with MBP-McbB, 10 mM magnesium acetate did not prevent the second zinc atom from binding and inhibiting heterocycle formation (Figure 4).

Formation of Apo-MBP-McbB. To investigate the role of zinc in the activity of McbB, several methods were used to remove the zinc, and heterocyclization activity was examined following reconstitution with the other synthetase subunits. Preliminary experiments indicated that activity was slowly lost when MBP-McbB was dialyzed with the chelator 1,10-phenanthroline over a time period of days, and that the subsequent level of zinc bound was undetectable (data not shown). However, this extensive dialysis also caused a noticeable decrease in the activity of the control sample even though it contained stoichiometric amounts of zinc (0.88). Attempts to restore activity by incubating the apo-protein with zinc were unsuccessful (data not shown).

By using the organomercurial compound PMPS, which efficiently ejects zinc from McbB (Figure 3), apo-protein could be prepared in a much shorter time. Apo-MBP-McbB containing less than 1% zinc was made by incubating the protein with excess PMPS for 30 min in the presence of EDTA, followed by the addition of 2 mM DTT. The PMPS was removed by dialyzing against multiple changes of buffer containing Chelex-100. The control sample treated under the same conditions in the absence of PMPS retained stoichiometric amounts of zinc. Incubation with the other synthetase components in the reconstitution assay revealed that the activity of the apo-protein was severely reduced. An example of such an experiment is shown in Figure 5A. This experiment was performed with subsaturating concentrations of MBP-McbB so that differences between the activity of protein samples could be detected.

Several attempts to restore enzyme activity by incubating apo-protein prepared as described for Figure 5A with zinc were unsuccessful (data not shown). It is possible that the apparent inability to reconstitute active holo-McbB from this apo-protein was due to the presence of the inhibitory binding site. However, even when the PMPS reaction was reversed in situ with DTT in the absence of EDTA, no significant enhancement in activity was detected (data not shown). In contrast, active holo-protein could be regenerated in situ if the PMPS reaction was reversed quickly (Figure 5B). MBP-McbB containing 4% zinc was produced when the protein was incubated with PMPS for a minute in the presence of EDTA, followed by the addition of DTT and extensive dialysis. If EDTA was omitted from the reaction, the protein was reconstituted with 88% zinc. Slightly longer reactions (1.5 min at room temperature instead of 1 min on ice) produced apo-protein with less than 1% zinc, and holo-protein could still be regenerated in the absence of EDTA (data not shown). The heterocyclization activity of the PMPS-treated holo-protein was similar to that of the control (Figure 5B). Testing the apo-protein in the reconstitution assay revealed that this protein also retained full activity. These experiments indicate that the PMPS does eject the zinc from MBP-McbB in this time frame but that the protein can rebind the metal in an active conformation if the PMPS−mercaptide bond is reversed quickly. After a few minutes, holo-protein cannot be regenerated, and the protein is irreversibly inactivated. Finally, the oxidation state of the cysteines was determined by using DTNB (Ellman's reagent) in the presence of 6 M guanidine hydrochloride. The wild-type protein was in a reduced state, an average of 5.4 $\pm$ 0.7 free

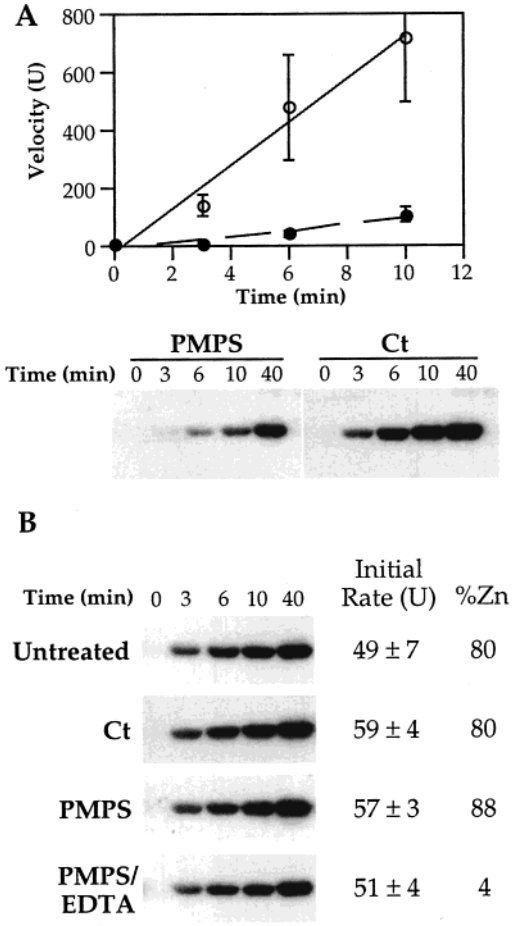

FIGURE 5: Activity of apo-MBP-McbB prepared with PMPS. (A) MBP-McbB was incubated either in the presence or in the absence of PMPS and EDTA over a period of 30 min, as described in Experimental Procedures, followed by the addition of DTT and metal-free dialysis. The activity of each sample was tested in reconstitution assays containing 0.5 μM MBP-McbB, 4 μM MBP-C, 4 μM thrombin-cleaved MBP-McbD, and 20 μM GGC, as described in Experimental Procedures. The error bars indicate the standard deviation between duplicate Western blots. The metal content of the samples, 0.3% for the PMPS-treated protein and 122% for the control (Ct) was measured by using ICP-MS. (B) MBP-McbB was incubated with PMPS in the presence or absence of EDTA for 1 min on ice prior to the addition of DTT. The control (Ct) sample was incubated with EDTA in the absence of PMPS. These samples were then dialyzed prior to metal analysis. The activity of each sample was tested in reconstitution assays as described for panel A, and the initial rate ± esd is listed for duplicate blots.

thiols were detected out of a possible total of six (Table 1). In contrast, the cysteines in the apo-protein prepared with either PMPS method were partially oxidized, with only 2−4 detectable thiols (data not shown).

MBP-McbB Mutants. Site-directed mutagenesis was used to replace potential zinc ligands with alanine. Each of the six cysteine residues were mutated, but C266A was insoluble and could not be purified. Of the other five mutants as well as the C181A/C184A double mutant, no activity was detected for C181A, C184A, C279A, C281A, or C181A/C184A when reconstituted with the other synthetase components (Table 1). These proteins all contained significantly reduced levels of zinc (30% or less). In addition, the inactive cysteine mutants were highly oxidized with only 1−3 detectable thiols. Only C269A was active, contained a stoichiometric amount of zinc, and had little oxidation of the cysteine residues.

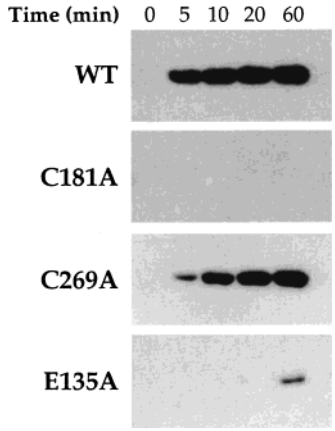

FIGURE 6: Heterocyclization activity of CBP-tagged MccB17 synthetases with mutations in the McbB subunit. Reactions containing 0.5 mg/mL protein and 20 μM GGC were incubated at 37 °C. Aliquots were removed at the indicated times, resolved on 10% SDS−polyacrylamide gels, and analyzed by Western blotting.

A few other alanine mutants were also constructed. If C181 and C184 are zinc ligands, homology with cytidine deaminase suggests that H133 is also a ligand (Figure 2) (*14*). Furthermore, the glutamate in cytidine deaminase that is homologous to E135 plays a significant role as a proton donor and acceptor (*15*). The H133A, E135A, and E135D mutants all had similar characteristics (Table 1). They contained substoichiometric amounts of zinc and oxidized cysteine residues, and the activity of these proteins in the reconstitution assay was undetectable (Table 1). In addition, T179, which is just upstream of the first CxxC motif, was changed to alanine, and the mutant was inactive and contained only about half of the normal amount of zinc. To test whether any disturbance in the primary structure would inactivate MBP-McbB, E102 was chosen at random and mutated to alanine. The protein was active with close to one zinc atom bound.

Certain McbB mutants were also examined in a calmodulin-binding peptide (CBP)-tagged version of the MccB17 synthetase (*9*). Although metal analysis is not possible in this system, the three components are coexpressed, which might increase the amount of properly folded protein and enhance the stability of the subunits. Furthermore, the complex is purified in a single step with the CBP tag on McbB, so the affects of the McbB mutations on subunit interactions can be monitored. Of the three McbB mutants investigated, the synthetases containing the C269A or E135A mutation eluted from the calmodulin column in a similar fashion as wild-type (data not shown). In contrast, the CPB-tagged C181A McbB subunit migrated on a gel as a doublet, and the McbD subunit was of such low abundance that it was undetectable. The heterocyclization activity of these complexes was tested by incubating the proteins with the MBP-McbA$_{1-46}$ (GGC) substrate followed by Western blot analysis (Figure 6). No activity was observed with the C181A mutant, but the C269A mutant exhibited a similar level of activity as the wild-type enzyme. These results reflect the activity of the corresponding MBP-McbB mutants. However, although no activity was observed with the E135A MBP-McbB mutant, very weak activity is detectable in the CBP-tagged enzyme.

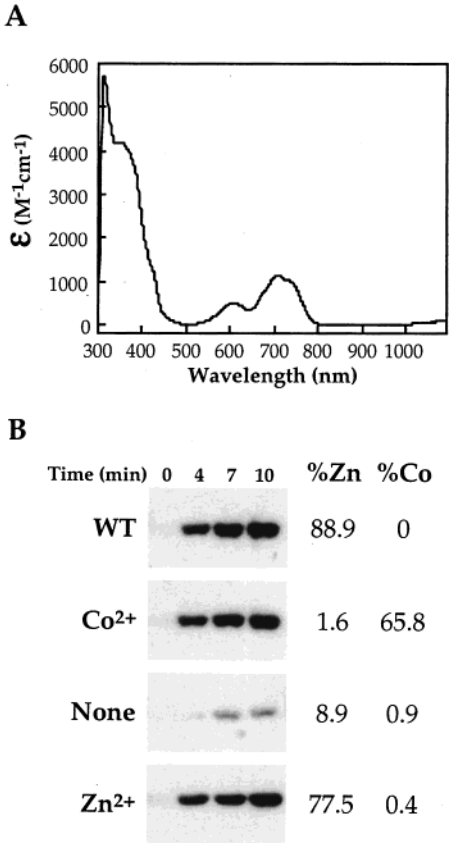

FIGURE 7: Cobalt(II)-substituted MBP-McbB. (A) The spectrum was generated by subtracting the spectrum of the zinc-containing protein expressed in LB and then correcting for the cobalt content (66%). (B) *E. coli* containing the MBP-McbB plasmid grown in metal-depleted minimal media were induced in the presence of 10 μM $CoCl_2$, in the presence of 10 μM $ZnSO_4$, or in the absence of any metals. The heterocyclization activity of the purified proteins was compared with that of MBP-McbB grown in LB (WT). Reconstitution assays containing 0.5 μM MBP-McbB, 4 μM MBP-McbC, 4 μM thrombin-cleaved MBP-McbD, and 20 μM GGC were incubated at 37 °C. Aliquots were removed at the indicated times, resolved on 10% SDS−polyacrylamide gels, and analyzed by Western blotting. The amount of zinc and cobalt bound was measured by using ICP emission spectrometry following metal-free dialysis.

Cobalt-Substituted MBP-McbB. One method used to study the metal coordination sphere of zinc-containing proteins is to replace the zinc with the paramagnetic probe cobalt(II) (*26*). The electronic absorption spectra of cobalt-substituted proteins are indicative of the type and number of metal ligands (*26*, *27*). However, the inability to put the zinc back into apo-McbB precluded replacing the zinc with any other metal. To produce cobalt-containing MBP-McbB, the protein was expressed in cells grown in metal-deficient minimal media containing 10 μM $CoCl_2$. This experiment was done several times, and protein containing up to 66% cobalt and as little as 1% zinc was produced. The experiments shown in Figure 7 were performed with protein expressed in 1 L of cells and purified only on an amylose column. Protein that was expressed on a larger scale and purified with an additional anion-exchange chromatography step had similar characteristics. An example of the UV−visible absorption spectrum is shown in Figure 7A. The position and intensities of the absorption bands are characteristic of a tetrathiolate coordination sphere (*27*). The intense band at 350 nm is indicative of charge transfer between Co(II) and sulfur

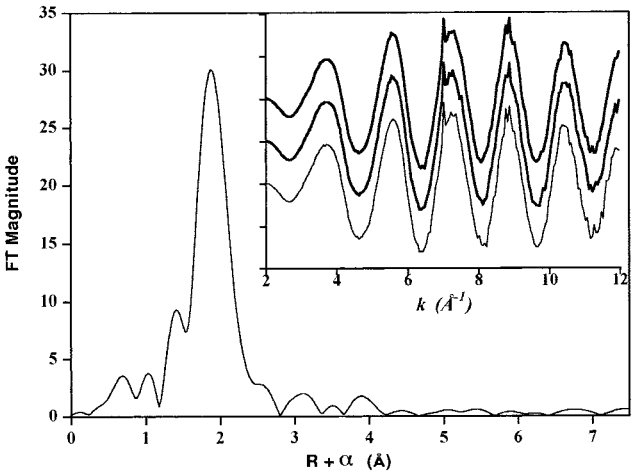

FIGURE 8: Fourier transform of EXAFS data for sample 3 (representative data). Inset: k^3-weighted EXAFS for all three samples.

Table 2: EXAFS Curve Fitting Results[a]

sample	coordination	R_{ab} (Å)[b]	σ^2 [c]	ϵ' ($\times 10^2$)[d]
1	4S	2.34	2.9	3.561
2	4S	2.34	2.9	3.937
3	4S	2.34	2.8	3.243

[a] Fits to filtered data. [b] Absorber−scatterer distance. [c] Debye−Waller factor ($\times 10^3$). [d] Fits are shown with best fit lowest ϵ' statistic, where ϵ' corrects for the number of variables in a fit, with $N_{idp} = (2\Delta k \Delta R)/\pi$ where Δk is k space over which the Fourier transform is taken, and ΔR is R space, which gives useful data in the back-transform. N_{var} is the number of variables in the fit. ϵ is the root mean square error between the data and the fit (*25*). $\epsilon' = \epsilon^2/(N_{idp} - N_{var})$.

ligands, and the extinction coefficient of 4200 M^{-1} cm^{-1} is in agreement with both model compounds and proteins that exhibit intensities of 900−1300 M^{-1} cm^{-1} per Co−S bond (*28*, *29* and references therein). In addition, the positions of the d−d transition bands, with maxima at 600 and 700 nm and a shoulder at 740 nm, are typical of other proteins containing tetrathiolate Co(II) sites such as metallothionein (*30*), a Cys_4 zinc finger (*31*), a methionyl-tRNA synthetase (*32*), and aspartate transcarbamoylase (*33*). All preparations of cobalt-substituted MBP-McbB exhibit similar levels of activity as the zinc-containing protein when tested in the reconstitution assay, an example of which is shown in Figure 7B. If no metal was added to the media, a small amount of protein was expressed, which contains very low amounts of zinc and exhibits barely detectable activity.

EXAFS Spectroscopy. Three samples of MBP-McbB were prepared for EXAFS (Figure 8). Sample 1 was from a different protein preparation than samples 2 and 3, and sample 3 was dialyzed against a Tris buffer rather than Hepes. All three samples gave the best fit for a single shell of four sulfurs, with a Zn−S distance of 2.34 Å and σ^2 values of 2.8−2.9 $\times$ 10^{-3} $Å^2$ (Table 2). In each case, fits using mixed ligation (e.g., 3S + 1N) gave poorer fits and had chemically unreasonable values for σ^2.

The data could also be fit assuming a total coordination number of 5. However, these fits were slightly worse and gave σ^2 values larger than expected (data not shown, *25*). The observed Zn−S distances are typical of a tetrahedral Zn and shorter than for pentacoordinate Zn.

EXAFS cannot distinguish directly between S and Cl scatterers. However, the observation of identical data for

samples prepared in Cl-free buffer and those prepared in 50 mM Tris-Cl suggests that chloride is not a zinc ligand. In addition, a ZnS_3Cl site would be expected to have a slightly shorter average Zn nearest neighbor distance and a larger σ^2 (*34*). Thus, the EXAFS data provide strong evidence for Zn−tetrathiolate ligation sphere, in accord with the UV−visible absorption spectra of the cobalt-containing protein.

DISCUSSION

The importance of zinc in vital processes is underscored by the fact that the study of zinc metalloproteins has encompassed members from all six classes of enzymes as well as a wide variety of other proteins (*15*, *35*). Although zinc is not redox active, it is functionally versatile due to the flexibility in coordination number, geometry, and type of ligands. The extensive literature on zinc-containing proteins has established that the metal environment is related to the function of the zinc ion, be it structural, catalytic, or regulatory (*15*, *36*). Thus, information on the metal requirements and coordination sphere of McbB may provide insight as to the role of zinc in the mechanism of oxazole and thiazole biosynthesis in the MccB17 production pathway.

The first step in this study was to determine the stoichiometry of zinc atoms bound to McbB. Multiple experiments under a variety of conditions established that purified MBP-McbB contains a single zinc atom. It was possible to load a second zinc on the protein, but this significantly diminished the heterocyclization activity of McbB when it was mixed with the other MccB17 synthetase components. Inhibition of a metalloenzyme by the binding of a second metal is not unprecedented (see ref *37* and references therein). For example, the zinc−proteinase carboxypeptidase A is competitively inhibited by zinc ions (*38*, *39*). Extensive biochemical studies and structural analysis of bovine pancreatic carboxypeptidase A confirmed that the second zinc binds a glutamate residue near the active site and that there is a hydroxide bridge between the catalytic and inhibitory zinc ions (*38*−*41*). Furthermore, it has recently been suggested that inhibitory zinc sites, in conjunction with thionein-mediated zinc removal and reactivation, could be a method for intracellular control of a variety of enzymatic pathways (*42*). Additional experiments are needed to determine where the second zinc binds in McbB and how the metal inhibits heterocycle formation.

Apo-MBP-McbB prepared with a 30-min incubation with PMPS resulted in a severely reduced rate of heterocycle formation, and incubation with zinc did not restore activity. However, if the PMPS reaction was reversed after only 1 min, the protein was able to rebind zinc with full activity. These experiments suggest that in this short time frame (1 min) the protein conformation does not significantly deteriorate, but that the apo-protein is not stable and slowly loses activity and the ability to bind zinc. In addition, one of the roles of the metal is to preserve the reduced form of the protein, although partial oxidation of the cysteine residues does not correlate with loss of activity. If the apo-protein is exposed to a reducing agent in a matter of minutes, the protein is stabilized and able to maintain an active conformation. A detailed structural analysis of the apo- and holoproteins may provide an explanation for this observation. These experiments also suggest that the zinc is not required for heterocyclization activity, but it is not possible to make that conclusion a rigorous one at the present time because the activity assays were not performed under metal-free conditions.

The structural instability of the individually expressed MccB17 synthetase components has been previously documented (*14*). It was only as fusions to the MBP tag that the three proteins could be separately expressed, purified, and then combined together to reconstitute heterocyclization activity. Thus it is not surprising that many of the site-directed mutations in MBP-McbB produced inactive protein, particularly since they were chosen on the basis of their potential to be metal ligands or to be involved in the mechanism of action. Some of the McbB mutants were also expressed and purified as the CBP-tagged synthetase complex. The inactivity of the C181A mutant and the activity of the C269A mutant reflects what was observed for the corresponding MBP-McbB proteins. The E135A mutant was initially examined because of the possibility that it corresponds to E104 of the *E. coli* cytidine deaminase, which serves an essential function as a protein shuttle (*15*, *43*). However, the E135A CBP-tagged mutant exhibits detectable heterocyclization activity, suggesting that although the E135A mutation causes enough structural disruption to inactivate the MBP fusion protein, it is not a zinc ligand or an integral part of the mechanism of action of the McbB subunit.

The spectroscopic analysis of the cobalt-containing protein and the EXAFS of the zinc-containing protein provide evidence for a tetrathiolate ligand sphere. All of the six cysteines in McbB were individually mutated to alanine and investigated as MBP fusions. Of the five that were purified, only the C269A mutant was active and contained a stoichiometric amount of zinc. The C266A mutant could not be analyzed because it was insoluble; however, previous studies have suggested that it is not required for heterocyclization (*14*). When MccB17-sensitive cells were exposed to crude extracts of cells expressing the whole MccB17 operon, extracts containing the C266A/C269A McbB mutant caused as much growth inhibition as did extracts containing the wild-type synthetase, suggesting that this mutant could produce equivalent amounts of mature MccB17. In contrast, the C181A and C184A McbB mutations appeared to block antibiotic production because no growth inhibition was observed. The results reported here, supplemented by these previous experiments, indicate that the zinc ligands of McbB are C181, C184, C279, and C281.

A zinc atom coordinated by four cysteine residues is found as a structural motif in a variety of proteins such as alcohol dehydrogenase, aspartate transcarbamoylase, and the protein families containing zinc-binding domains such as zinc fingers, GAL4 domains, RING domains, and LIM domains (*44*−*46*). The importance of the zinc in these proteins is likely due to its control over the local conformation, resulting in well-defined structures that modulate interactions with other cellular factors. For example, many genetic regulators contain zinc-finger domains, and studies have focused on the affinity of this polypeptide motif for nucleic acids (*47*). Recently, however, it has become clear that zinc fingers also mediate protein−protein interactions (*48*). Similarly, the only common characteristic noted in RING domain-containing proteins, which are found in a wide range of cellular

pathways, is their ability to bind to other proteins and their involvement in large multi-protein complexes (*46*). Thus the zinc-binding structure of McbB may be involved in the assembly of the MccB17 synthetase or possibly in binding the McbA peptide during heterocyclization.

Given the results described in this paper, it is less likely that the zinc in McbB is directly involved in heterocyclization of McbA during the production of mature MccB17 antibiotic, as suggested in Figure 2B. In general, the coordination sphere of a catalytic zinc site consists of three protein residues and water (*15*, *44*). There are exceptions to this rule, however (*49*). Further study is needed to determine if the zinc in McbB plays any catalytic role in the MccB17 synthetase, and indeed what capacity the McbB subunit fills in the conversion of 14 residues in the McbA substrate to the eight heterocycles of the antibiotic product.

ACKNOWLEDGMENT

We thank Dr. Jill C. Milne for the construction of several of the MBP-McbB mutants as well as for helpful advice. We are also grateful to Dr. Ranabir Sinha Roy, Dr. Florian Hollfelder, and Dr. Brian Hubbard for many discussions.

REFERENCES

1. Sinha Roy, R., Gehring, A. M., Milne, J. C., Belshaw, P. J., and Walsh, C. T. (1999) *Nat. Prod. Rep. 16*, 249−263.
2. Jack, R. W., and Jung, G. (1998) *Chimia 52*, 48−55.
3. Yorgey, P., Lee, J., Kördel, J., Vivas, E., Warner, P., Jebaratnam, D., and Kolter, R. (1994) *Proc. Natl. Acad. Sci. U.S.A. 91*, 4519−4523.
4. Bayer, A., Freund, S., and Jung, G. (1995) *Eur. J. Biochem. 234*, 414−426.
5. Moreno, F., San Millán, J. L., Hernández-Chico, C., and Kolter, R. (1995) in *Genetics and Biochemistry of Antibiotic Production* (Vining, L. C., and Stuttard, C., Eds.) pp 307−321, Butterworth-Heinemann, Boston.
6. Li, Y.-M., Milne, J. C., Madison, L. L., Kolter, R., and Walsh, C. T. (1996) *Science 274*, 1188−1193.
7. Madison, L. L., Vivas, E. I., Li, Y.-M., Walsh, C. T., and Kolter, R. (1997) *Mol. Microbiol. 23*, 161−168.
8. Sinha Roy, R., Kim, S., Baleja, J. D., and Walsh, C. T. (1998) *Chem. Biol. 5*, 217−228.
9. Sinha Roy, R., Belshaw, P. J., and Walsh, C. T. (1998) *Biochemistry 37*, 4125−4136.
10. Kelleher, N. L., Belshaw, P. J., and Walsh, C. T. (1998) *J. Am. Chem. Soc. 120*, 9716−9717.
11. Belshaw, P. J., Sinha Roy, R., Kelleher, N. L., and Walsh, C. T. (1998) *Chem. Biol. 5*, 373−384.
12. Kelleher, N. L., Hendrickson, C. L., and Walsh, C. T. (1999) *Biochemistry 38*, 15623−15630.
13. Milne, J. C., Eliot, A. C., Kelleher, N. L., and Walsh, C. T. (1998) *Biochemistry 37*, 13250−13261.
14. Milne, J. C., Sinha Roy, R., Eliot, A. C., Kelleher, N. L., Wokhlu, A., Nickels, B., and Walsh, C. T. (1999) *Biochemistry 38*, 4768−4781.
15. Lipscomb, W. N., and Sträter, N. (1996) *Chem. Rev. 96*, 2375−2433.
16. Vizán, J. L., Hernández-Chico, C., del Castillo, I., and Moreno, F. (1991) *EMBO J. 10*, 467−476.
17. Yorgey, P., Davignino, J., and Kolter, R. (1993) *Mol. Microbiol. 9*, 897−905.
18. Hunt, J. B., Neece, S. H., Schachman, H. K., and Ginsburg, A. (1984) *J. Biol. Chem. 259*, 14793−14803.
19. Hunt, J. B., Neece, S. H., and Ginsburg, A. (1985) *Anal. Biochem. 146*, 150−157.
20. Giedroc, D. P., Keating, K. M., Williams, K. R., Konigsberg, W. H., and Coleman, J. E. (1986) *Proc. Natl. Acad. Sci. U.S.A. 83*, 8452−8456.
21. Griep, M. A., and Lokey, E. R. (1996) *Biochemistry 35*, 8260−8267.
22. *International Tables for X-Ray Crystallography* (1962) (MacGillavry, C. H., and Rieck, G. D., Eds.) Vol. 3, The Kynoch Press, Birmingham.
23. Rehr, J. J., Mustre de Leon, J., Zabinsky, S. I., and Albers, R. C. (1991) *J. Am. Chem. Soc. 113*, 5135−5140.
24. Rehr, J. J., Albers, R. C., and Zabinsky, S. I. (1992) *Phys. Rev. Lett. 69*, 3397−3400.
25. Clark-Baldwin, K., Tierney, D. L., Govindaswamy, N., Gruff, E. S., Kim, C., Berg, J., Koch, S. A., and Penner-Hahn, J. E. (1998) *J. Am. Chem. Soc. 120*, 8401−8409.
26. Maret, W., and Vallee, B. L. (1993) *Methods Enzymol. 226*, 52−71.
27. Bertini, I., and Luchinat, C. (1984) in *Advances in Inorganic Biochemistry* (Eichorn, G. L., and Marzilli, L. G., Eds.) pp 71−111, Elsevier Science Publishers, New York.
28. Lane, R. W., Ibers, J. A., Frankel, R. B., Papaefthymiou, G. C., and Holm, R. H. (1977) *J. Am. Chem. Soc. 99*, 84−97.
29. May, S. W., and Kuo, J.-Y. (1978) *Biochemistry 17*, 3333−3338.
30. Good, M., and Vašák, M. (1986) *Biochemistry 25*, 3328−3334.
31. Shi, Y., Beger, R. D., and Berg, J. (1993) *Biophys. J. 64*, 749−753.
32. Landro, J. A., and Schimmel, P. (1993) *Proc. Natl. Acad. Sci. U.S.A. 90*, 2261−2265.
33. Johnson, R. S., and Schachman, H. K. (1983) *J. Biol. Chem. 258*, 3528−3538.
34. Brown, I. D., and Altermatt, D. (1985) *Acta Crystallogr. B41*, 244−247.
35. Vallee, B. L., and Falchuk, K. H. (1993) *Physiol. Rev. 73*, 79−118.
36. Christianson, D. W. (1991) *Adv. Protein Chem. 42*, 281−355.
37. Louie, A. Y., and Meade, T. J. (1999) *Chem. Rev. 99*, 2711−2734.
38. Larsen, K. S., and Auld, D. S. (1989) *Biochemistry 28*, 9620−9625.
39. Larsen, K. S., and Auld, D. S. (1991) *Biochemistry 30*, 2613−2618.
40. Gomez-Ortiz, M., Gomis-Rüth, F. X., Huber, R., and Avilés, F. X. (1997) *FEBS Lett. 400*, 336−340.
41. Bukrinsky, J. T., Bjerrum, M. J., and Kadziola, A. (1998) *Biochemistry 37*, 16555−16604.
42. Maret, W., Jacob, C., Vallee, B. L., and Fischer, E. H. (1999) *Proc. Natl. Acad. Sci. U.S.A. 96*, 1936−1940.
43. Xiang, S., Short, S. A., Wolfenden, R., and Carter, C. W. J. (1997) *Biochemistry 36*, 4768−4774.
44. Vallee, B. L., and Auld, D. S. (1990) *Biochemistry 29*, 5647−5659.
45. Berg, J. M., and Shi, Y. (1996) *Science 271*, 1081−1085.
46. Borden, K. L. B. (2000) *J. Mol. Biol. 295*, 1103−1112.
47. Klug, A., and Schwabe, J. W. R. (1995) *FASEB J. 9*, 597−604.
48. Mackay, J. P., and Crossley, M. (1998) *Trends Biochem. Sci. 23*, 1−4.
49. Matthews, R. G., and Goulding, C. W. (1997) *Curr. Opin. Chem. Biol. 1*, 332−339.

BI001398E